4182–4190 *Nucleic Acids Research, 2005, Vol. 33, No. 13*
doi:10.1093/nar/gki722

Preferential binding of a G-quadruplex ligand to human chromosome ends

Christine Granotier[1], Gaëlle Pennarun[1,2], Lydia Riou[1], Françoise Hoffschir[1], Laurent R. Gauthier[1], Anne De Cian[2], Dennis Gomez[4], Eliane Mandine[3], Jean-François Riou[4], Jean-Louis Mergny[2], Patrick Mailliet[3], Bernard Dutrillaux[1] and François D. Boussin[1,*]

[1]LRP, DRR, CEA, 92265 Fontenay-aux-Roses, France, [2]Laboratoire de Biophysique, INSERM U565, CNRS UMR 5153, Muséum National d'Histoire Naturelle USM 503, 75005 Paris, France, [3]Aventis Pharma SA, Centre de Recherche de Paris, 94403 Vitry-sur-Seine, France and [4]Laboratoire d'Onco-Pharmacologie, JE 2428, Université de Reims Champagne-Ardenne, 51096, Reims, France

Received April 19, 2005; Revised June 17, 2005; Accepted July 5, 2005

ABSTRACT

The G-overhangs of telomeres are thought to adopt particular conformations, such as T-loops or G-quadruplexes. It has been suggested that G-quadruplex structures could be stabilized by specific ligands in a new approach to cancer treatment consisting in inhibition of telomerase, an enzyme involved in telomere maintenance and cell immortality. Although the formation of G-quadruplexes was demonstrated *in vitro* many years ago, it has not been definitively demonstrated in living human cells. We therefore investigated the chromosomal binding of a tritiated G-quadruplex ligand, ^{3}H-360A (2,6-*N*,*N*′-methyl-quinolinio-3-yl)-pyridine dicarboxamide [methyl-^{3}H]. We verified the *in vitro* selectivity of ^{3}H-360A for G-quadruplex structures by equilibrium dialysis. We then showed by binding experiments with human genomic DNA that ^{3}H-360A has a very potent selectivity toward G-quadruplex structures of the telomeric 3′-overhang. Finally, we performed autoradiography of metaphase spreads from cells cultured with ^{3}H-360A. We found that ^{3}H-360A was preferentially bound to chromosome terminal regions of both human normal (peripheral blood lymphocytes) and tumor cells (T98G and CEM1301). In conclusion, our results provide evidence that a specific G-quadruplex ligand interacts with the terminal ends of human chromosomes. They support the hypothesis that G-quadruplex ligands induce and/or stabilize G-quadruplex structures at telomeres of human cells.

INTRODUCTION

Telomeres, the nucleoprotein structures at the end of eukaryotic chromosomes, are essential for chromosome replication and the prevention of chromosome degradation and fusion. They are maintained by telomerase, a specific reverse transcriptase. The catalytic subunit of this enzyme, hTERT, uses its RNA subunit (hTR) as a matrix for the addition of GGTTAG telomere repeats to the 3′ ends of chromosomes. Telomerase, the expression of which is repressed in most somatic human cells, is reactivated in most tumors (90%) and is thought to enable cancer cells to proliferate in an unlimited manner, by maintaining and protecting telomeres (1,2). Telomerase has, therefore, become a target for the development of new anticancer drugs (3). Various classes of telomerase inhibitors have been developed in recent years (4,5). G-quadruplex ligands target the telomeres rather than telomerase itself. Indeed, structure studies (X-ray crystallography and nuclear magnetic resonance) of oligonucleotides have indicated that the single-stranded telomeric-3′-overhang could adopt a variety of quadruplex structures based on four Hoogsteen-paired coplanar guanines (6–8). Various G-quadruplex ligands have been shown to inhibit telomerase *in vitro*. Some of these molecules have also been shown to induce telomere shortening and/or instability, triggering apoptosis and/or senescence programs in various cell lines (9–15). However, the precise mechanism of action of these molecules remains unclear: despite the fact that the existence of G-quadruplexes was shown *in vitro* many

*To whom correspondance should be addressed. Tel: +33 1 46 54 97 91; Fax: +33 1 46 54 97 02; Email: boussin@cea.fr

The authors wish it to be known that, in their opinion, the first two authors should be regarded as joint First Authors

years ago, it has not been definitively demonstrated that G-quadruplexes exist *in vivo*, except in ciliates (16) and *Escherichia coli* (17). Although it has been proposed that G-quadruplexes exist *in vivo* in the promoter of *c-myc* (18) and at telomeres (19), their existence in human cells is still a matter of debate.

In this study, we investigated the targeting in human cells of 360A (2,6-*N*,*N*′-methyl-quinolinio-3-yl-pyridine dicarboxamide), a member of a new family of pyridine derivatives that interact highly selectively *in vitro* with G-quadruplexes compared with double-stranded DNA and inhibit telomerase activity (15,20). This G-quadruplex ligand induces delayed growth arrest followed by massive apoptosis in various immortalized cell lines in direct correlation with telomeric instability (15). We used tritiated-360A to investigate the behavior of this compound in various cell types. We first checked the *in vitro* selectivity for G-quadruplex structures by equilibrium dialysis. Then, we showed by *in vitro* binding experiments with human genomic DNA that ^{3}H-360A has a very potent selectivity toward G-quadruplex structures of the telomeric G-overhang. Finally, we showed by autoradiography of metaphase spreads that tritiated-360A was preferentially bound to terminal regions of chromosomes of both human normal cells and immortalized cell lines.

MATERIALS AND METHODS

Chemical compounds

We used a 90.4% pure solution of tritiated-360A (^{3}H-360A; 2,6-*N*,*N*′-methyl-quinolinio-3-yl)-pyridine dicarboxamide [methyl-^{3}H] di-iodide, formula shown in Figure 1A) in 50% aqueous ethanol, with a specific activity of 163 Ci/mmol. The unlabeled compound, 360A, belongs to a series of 2,6-pyridine-dicarboxamide derivatives displaying strong affinity and selectivity for G-quadruplex structures and selective telomerase inhibition in *in vitro* assays (15).

Equilibrium dialysis

We used 400 ml of the dialysate solution containing 130 µCi ^{3}H-360A for each competition dialysis assay. We pipetted 200 µl of a 75 µM solution of the monomeric unit (nucleotide, base pair, base triplet or quartet) of each of the nucleic acid samples (fully described in Table 1) into a separate dialysis unit (Pierce). All 19 dialysis units were then placed in a beaker containing the dialysate solution—15 mM sodium cacodylate (pH 6.5), 10 mM $MgCl_2$ and 185 mM NaCl. This assay has been described in more detail elsewhere (21). The beaker was covered with Parafilm, wrapped in aluminum foil, and its contents were allowed to equilibrate overnight at room temperature (20–22°C), with continuous stirring. DNA samples were then carefully transferred to microfuge tubes, and the radioactivity in each chamber was determined with an LKB Wallac 1211 Rackbeta apparatus (mean of two independent experiments, each counted twice). The radioactivity signal is normalized by the signal obtained in a control chamber that only contains buffer. Binding of the ligand to a nucleic acid sample leads to an accumulation of the ligand in the chamber and therefore to an increased normalized radioactivity signal.

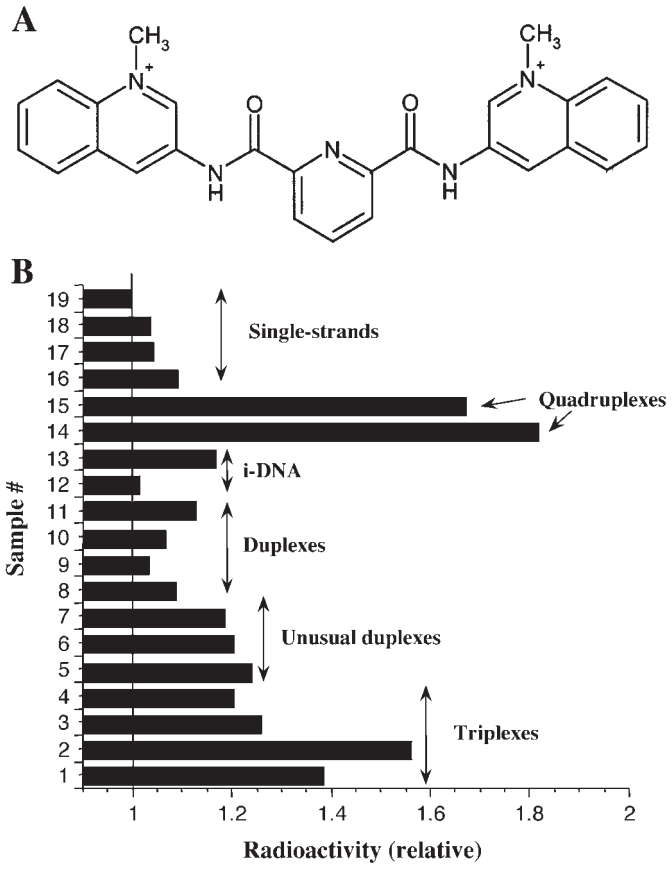

Figure 1. Structural selectivity of ^{3}H-360A as assessed by equilibrium dialysis. (**A**) Chemical formula of the compound. (**B**) Accumulation of tritiated-360A in each dialysis unit. The normalized radioactivity value of '1' corresponds to the signal obtained in an empty chamber (no DNA; passive diffusion of the radioactive ligand through the dialysis membrane). Binding of the ligand to a nucleic acid sample is indicated by a higher than one normalized radioactivity signal. ^{3}H-360A preferentially binds *in vitro* to quadruplexes, rather than to duplexes or single strands. The 19 oligo and poly-nucleotide samples used in these experiments are described in Table 1.

In vitro binding to purified genomic DNA

Aliquots of 2 µg of undigested genomic DNA from A549 cells were incubated at 50°C overnight with 1 nM (final concentration) of ^{3}H-360A in buffer containing 20 mM Tris, pH 8.0, 50 mM NaCl and 1 mM EDTA in a volume of 20 µl in the presence or absence of competitor oligonucleotides (1 µM), as indicated. Reactions were stopped by the addition of 6 µl of loading buffer (20% glycerol, 1 mM EDTA and 0.2% bromophenol blue), and samples were electrophoresed on 0.8% agarose gels in 1× TBE buffer containing ethidium bromide (Et-Br). Gels were dried on Whatman filter paper. Et-Br fluorescence and radioactivity were scanned with a PhosphorImager (Thyphoon 9210, Amersham Biosciences). Results were expressed as the relative binding signal normalized to the fluorescent signal of Et-Br and represented at least three independent experiments.

Cells

All cells were cultured at 37°C, in an atmosphere containing 5% CO_2. CEM1301 cells (T-cell lymphoblastic leukemia; DAKO) were cultured at a density of 5×10^{5}/ml in

Table 1. Sequence of the oligo- and poly-nucleotides used in equilibrium dialysis

Number	Name	Sequence
#1	(T,C) TRIPLEX	TT-CTTTCTCTCCTCC-3′ *5′-GAAAGAGAGGAGG-3′* CC-CTTTCTCTCCTCC-5′
#2	(G,A) TRIPLEX	TT-GGAGGAGAGAAAG-3′ CC-GGAGGAGAGAAAG-5′ *5′-CCTCCTCTCTTTC-3′*
#3	(G,T) TRIPLEX	TT-GGTGGTGTGTTTG-3′ CC-GGAGGAGAGAAAG-5′ *5′-CCTCCTCTCTTTC-3′*
#4	Poly(dA).2 poly(dT)	...TTTTTTTTTTTTT...-3′ ...AAAAAAAAAAAAA...-5′ *...TTTTTTTTTTTTT...-3′*
#5	24GA (parallel duplex)	5′-GAGAGAGAGAGAGAGAGAGAGAGA-3′
#6	psD duplex	5′-AAAAAAAAAATAATTTTAAATATT-3′ 5′-TTTTTTTTTTATTAAAATTTATAA-3′
#7	24CTG	5′-CTGCTGCTGCTGCTGCTGCTGCTG-3′
#8	Poly(dA–dT)	...ATATATATATATA...-3′ (double-stranded DNA polymer) ...TATATATATATAT...-5′
#9	Poly(dG–dC)	...GCGCGCGCGCGCG...-3′ (double-stranded DNA polymer) ...CGCGCGCGCGCGC...-5′
#10	Calf thymus DNA	(double-stranded DNA polymer, mixed sequence)
#11	ds 26	5′-CAATCGGATCGAATTCGATCCGATTG-3′
#12	Poly (dC)	5′-...CCCCCCCCCCCCC...-3′ (DNA polymer)
#13	22CT	5′-CCCTAACCCTAACCCTAACCCT-3′
#14	22AG	5′-AGGGTTAGGGTTAGGGTTAGGG-3′
#15	24G20	5′-TTGGGGGGGGGGGGGGGGGGGGTT-3′
#16	Poly(dT) (single-stranded)	5′-...TTTTTTTTTTTTT...-3′ (DNA polymer)
#17	Poly(dA) (single-stranded)	5′-...AAAAAAAAAAAAA...-3′ (DNA polymer)
#18	Poly(rU) (single-stranded)	5′r-...UUUUUUUUUUU...-3′ (RNA polymer)
#19	Poly(rA) (single-stranded)	5′r-...AAAAAAAAAAAA...-3′ (RNA polymer)

RPMI-1640 (Sigma) supplemented with 10% decomplemented fetal calf serum (FCS) (Invitrogen), 2 mM glutamine (Sigma) and penicillin–streptomycin (Sigma). Human glioma T98G cells were cultured in DMEM (Invitrogen) supplemented with 10% FCS, 2 mM glutamine and antibiotics. Peripheral blood lymphocytes (PBLs) were isolated from blood samples from normal volunteers (CEN-FAR infirmary) by centrifugation with Histopaque (Sigma) and cultured at a density of 10^6/ml in M199 medium (Invitrogen) supplemented with 24% FCS and 1.2% phytohemagglutinin (PHA)-C (Bio-Sepra).

Metaphase preparations and autoradiography

The protocol used was derived from a previously described method (22). Metaphases were prepared from cells cultured in their specific medium supplemented with 0.3 μM ^{3}H-360A at 37°C, in a humidified atmosphere containing 5% CO_2. After various times, cells were incubated with colcemid (0.04 μg/ml; Sigma) at 37°C for 40 min (CEM1301 and T98G) or 2 h (PBL). They were then centrifuged (after trypsin treatment for T98G) at 1500 r.p.m. (GR422, Jouan) for 5 min and the supernatant was discarded. Warmed hypotonic solution was added to the cell pellet, which was resuspended by gentle pipetting, and the resulting suspension was incubated at 37°C for 20 min. The cell suspension was centrifuged at 1400 r.p.m. for 7 min. The pellet was resuspended and fixed by vortexing twice in ethanol:acetic acid (3:1 mixture) and was stored overnight at 4°C. The suspension was applied on cold wet slides by means of a dropper for chromosome preparations. The slides were air-dried overnight. Slides were then incubated in 2× SSC supplemented with 0.1 mg/ml RNase A (Sigma) for 1 h at 37°C. Slides were washed and dehydrated by successive ethanol baths and were then air-dried. They were dipped into Kodak NTB2 nuclear emulsion, developed after exposure for 2 days and stained with Mayer's hemalum (Merck). Metaphases were captured with an Olympus BX51 microscope. We counted the number of silver grains suggestive of a telomeric location for the radioactive compounds (i.e. covering at least part of the end of a chromatid), and the number of grains covering other regions of the chromosomes for at least 50 metaphases. The number of silver grains in terminal and interstitial areas was compared with the total number of grains in the metaphase areas. We estimated the areas of the metaphases and the areas in which a grain was considered to cover a terminal or interstitial region of the chromosome by means of Metamorph software (Universal Imaging

Corporation), making it possible to determine silver grain densities over the various regions. We compared the mean values obtained statistically by means of *t*-tests (Statview, Abacus Concept Inc.).

RESULTS

In vitro selectivity of ^{3}H-360A for G-quadruplex structures

The selectivity of ^{3}H-360A for G-quadruplex structures was checked by competitive equilibrium dialysis (Figure 1B). The sequence and structural selectivity of various DNA binding agents was previously explored using a thermodynamically rigorous competition dialysis procedure (23). With this method, various nucleic acid structures are dialyzed against a common ligand solution. The amount of ligand accumulated in the dialysis tube is highest for the tube containing the structural form with the highest ligand-binding affinity (23), and the amount of dye bound to a given structure can be correlated with the affinity of the dye for that sample. We designed a set of 19 nucleic acid structures (24), ranging from single strands to G- or C-quadruplexes, and analyzed the binding of ^{3}H-360A to these structures. The binding pattern of the equilibrium dialysis for ^{3}H-360A was very similar to the one of the non-radioactive 360A ligand (data not shown). The tritiated compound accumulated in the two chambers corresponding to DNA quadruplexes (# 14 and 15), but displayed only minimal binding to regular double-stranded (# 8–11) or single-stranded (# 16–19) samples. This confirms that the tritiated ligand bound preferentially to quadruplex structures (intra- or intermolecular).

However, there was also a significant binding to some triplex structures, such as the GT and GA triplexes. The relative affinity toward quadruplexes was only 1.5- to 2-fold higher than the affinity for these triplexes. We noticed that these two triplexes involved guanine-rich strands (5′-GAAAGAGAGGAGGCCTTGGAGGAGAGAAAG and 5′-GAAAGAGAGGAGGCCTTGGTGGTGTGTTTG) hybridized to a short pyrimidine strand (CCTCCTCTCTTTC). Therefore, we anticipated that the quadruplex ligand could have disrupted these triplexes and bound to the purine-rich strands in a quadruplex conformation. To test this hypothesis, we performed a similar dialysis experiment in which binding to triplexes GA and GT was compared with binding to the GA and GT strands (i.e. in the absence of the short pyrimidine oligomer required for triplex formation). Binding to the GA and GT strands alone was similar to binding to GA and GT triplexes (data not shown), strongly suggesting that the apparent strong binding to triplexes is artefactual, and results from a conversion to a quadruplex in the presence of the ligand. Finally, we checked that binding to double-stranded telomeric DNA was minimal, using two different sequences: an intramolecular double-stranded hairpin with two GGGTTA repeats and an intermolecular 5′ d(GGGTTA)$_3$GGG/5′ d-(CCCTAA)$_3$CCC duplex (data not shown).

^{3}H-360A specifically binds to telomeric G-overhang from purified genomic DNA

We next studied the binding of ^{3}H-360A to purified genomic DNA. Overnight incubation of 1 nM ^{3}H-360A with 2 µg genomic DNA from A549 cells followed by native agarose gel electrophoresis allowed to detect the radioactive signal of the compound at the position of undigested genomic DNA as a single band (Figure 2B). To determine whether such ligand has a preference for telomeric sequences, competition experiments with various oligonucleotides (1 µM) were performed (Figure 2A). As controls, T7 single-stranded oligonucleotide and 21Tel double-stranded telomeric repeats did not change the binding of the ligand (Figure 2B and C). In contrast, a competition with the G-quadruplex-forming oligonucleotide 21G abolished the ^{3}H-360A signal (upper band in Figure 2B and 2C) and most of the ^{3}H-360A radioactivity was detected at the position of the oligonucleotide (bottom band, Figure 2D). A related control sequence (21Gmu3) which is

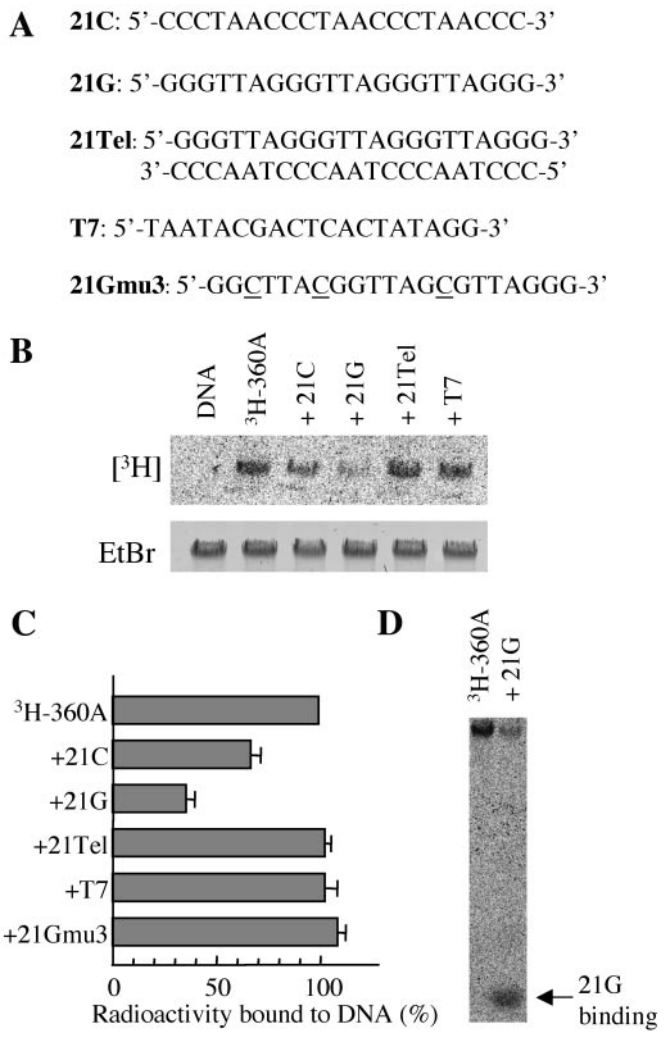

Figure 2. Specific binding of ^{3}H360A to telomeric G-overhang. (**A**) Sequence of the oligonucleotide competitor used. (**B**) Binding of ^{3}H-360A (1 nM) to purified A549 genomic DNA after agarose gel electrophoresis in the absence or presence of 1 µM oligonucleotide competitors (+21C, +21G, +21Tel, +T7) or DNA, control DNA without ^{3}H-360A. [^{3}H], radioactive signal of the gel; Et-Br, ethidium bromide staining of the gel. (**C**) Quantification of the ^{3}H-360A binding to the genomic DNA. The radioactivity signal is normalized relative to the Et-Br signal, defined as 100% for 1 nM ^{3}H-360A without competitors. The results corresponded to at least three independent experiments (mean ± SD). (**D**) In the presence of 21G (1 µM), most of the ^{3}H360A radioactivity was detected at the position of the oligonucleotide (indicated by an arrow at the bottom of the gel).

unable to form a G-quadruplex did not compete with the ^{3}H-360A binding, indicating that ^{3}H-360A has a preference for G-quadruplex.

Interestingly, the addition of 21C that hybridized to the telomeric G-overhang and masked the single-stranded part of telomeric ends decreased the binding of ^{3}H-360A to 65% of the initial signal (Figure 2B and C). This result suggests that at least 35% of ^{3}H-360A binding to the genomic DNA indeed corresponds to a specific binding to the telomeric G-overhang.

All together these results confirm the relative specificity of ^{3}H-360A for G-quadruplexes. They also suggest that roughly one-third of the ^{3}H-360A binding to the genomic DNA corresponded to a specific binding to the telomeric G-overhang. The huge molar excess of double-stranded compared with single-stranded telomeric sequences in the context of a whole genome could suggest that ^{3}H-360A has a strong preference for the telomeric G-overhang.

Preferential binding of ^{3}H-360A to terminal regions of chromosomes in immortalized tumor cells with short telomeres

We have shown previously that treatment of T98G (a glioblastoma cell line with short telomeres <4 kb) by 360A induced apoptosis in direct correlation with telomeric instability (15) (data not shown). Autoradiographs of T98G cells cultured with 0.3 μM ^{3}H-360A for 6–72 h revealed that the tritiated compound entered the cells within 6 h after the start of treatment and progressively accumulated in the nuclei of living cells without any permeabilization treatment (Figure 3A and B).

We then investigated the sites to which the compound bound on genomic DNA by autoradiography of metaphase spreads of T98G treated with ^{3}H-360A. We observed only very small numbers of silver grains on autoradiographs from untreated cultures (Figure 3C and E), enabling us to ignore this background noise for the interpretation of the data obtained with the tritiated compound (Figure 3D). Autoradiographs of T98G cells cultured with ^{3}H-360A showed that grains were preferentially located on the chromosomes (Figure 3D), indicating that this compound bound to genomic DNA sequences. Silver grains were located both at the ends of the chromosomes (black arrows, referred to here as terminal regions) and on other chromosomal regions (red arrows, referred to here as interstitial regions). We compared the putative binding of this compound to telomeres with that to other regions of chromosomes by separately counting the grains on the ends of the chromosomes and those on interstitial regions from 50 metaphases prepared after 24, 48 and 72 h of culture with the

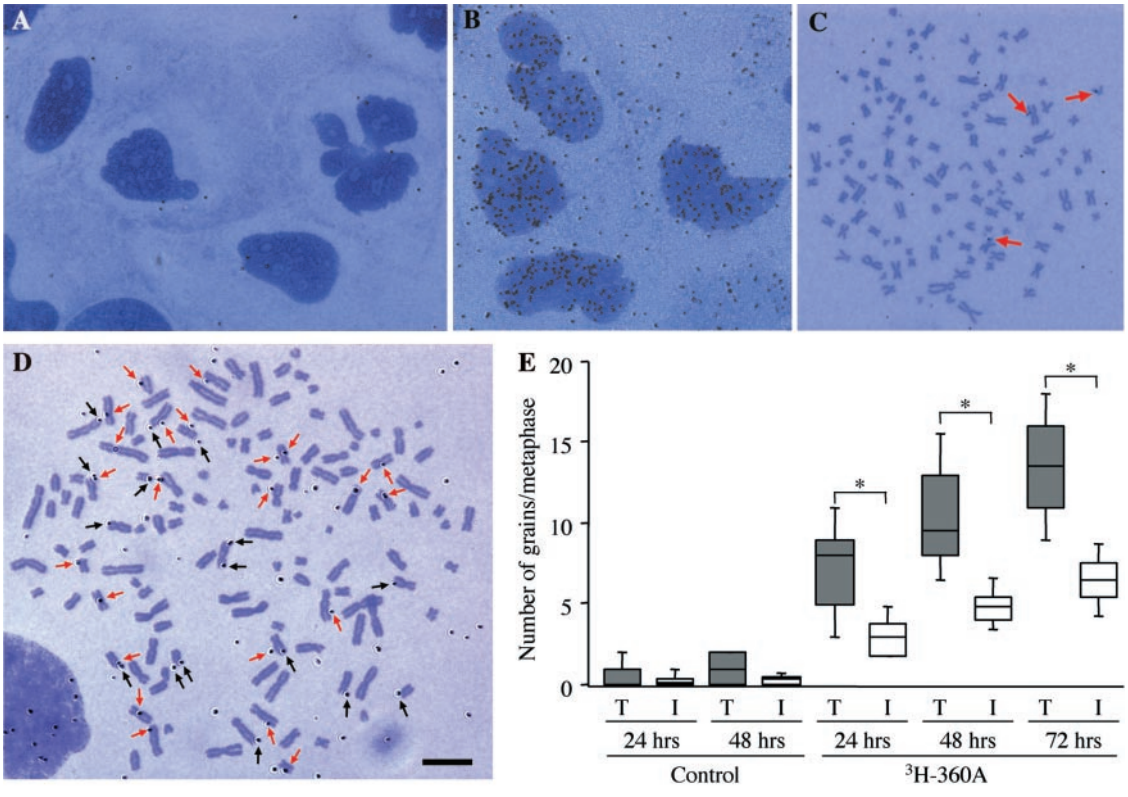

Figure 3. Detection of ^{3}H-360A by autoradiography in T98G cells. (**A** and **B**) Autoradiographs of T98G cultured without (A) or with (B) ^{3}H-360A for 24 h, showing accumulation of the radioactive compound in nuclei. Nuclei were stained with Mayer's hemalum solution. (**C** and **D**) Autoradiographs of metaphase spreads of T98G cells cultured without (C) or with (D) ^{3}H-360A for 48 h. Black arrows indicate silver grains on the terminal regions and red arrows indicate silver grains on the interstitial regions. Bars = 10 μm. (**E**) Densities of silver grains on the terminal (*T*) and interstitial (*I*) regions of chromosomes. Silver grains were counted in 25 metaphases/group for untreated controls and 50 metaphases/group for cultures with ^{3}H-360A. *I* values were normalized to areas of terminal regions by dividing the total numbers of grains on interstitial regions in each metaphase by the mean ratio of interstitial and terminal areas estimated with Metamorph software (2.93 ± 0.44 at 24 h, $n = 20$; 3.52 ± 0.48 at 48 h, $n = 20$; 3.34 ± 0.29 at 72 h, $n = 20$). Boxes include 50% of the values centered on the median (the horizontal line through the box). The vertical lines begin at the 10th percentile and end at the 90th percentile. *T* values are significantly greater than *I* values: *, *t*-test: $P < 0.0001$. Similar results were reproduced with another batch of the tritiated compound.

tritiated compound (Figure 3E). The areas covered by silver grains on the interstitial and terminal regions differed in size; we therefore determined the ratio of these areas with Metamorph software and used this ratio to compare the densities of silver grains on the terminal and interstitial regions for each metaphase.

The densities of silver grains on the terminal and interstitial regions increased over time, consistent with nuclear accumulation of the compound. At all incubation times, silver grain density was significantly higher at the ends of the chromosomes than at the interstitial regions (Figure 3E). These data suggest that the radioactive compound preferentially bound to the terminal regions of chromosomes, in accordance with the hypothesis of a preferential binding of ^{3}H-360A to telomeres.

^{3}H-360A is naturally unstable due to progressive radiolysis, and the batches should be used within the first few weeks after synthesis in order to be able to analyze the properties of the intact compound. To perform an additional control of our autoradiography experiments, we thus used a degraded batch of ^{3}H-360A that had lost most of its ability to bind G-quadruplex structures as shown by equilibrium dialysis (Supplementary Figure 1A). T98G cells were treated for 24 h with this degraded compound and autoradiographies of metaphases were analyzed using the same method than that used for the cells treated with the fresh compound. Results showed no preferential localization of the degraded radioactive compounds on terminal regions compared with interstitial regions of chromosomes (Supplementary Figure 1B) confirming the results obtained with the 'fresh' ^{3}H-360A.

Preferential binding of ^{3}H-360A to terminal regions of chromosomes in immortalized tumor cells with very long telomeres

We repeated these experiments with CEM1301 cells, a T-lymphoblastic cell line with very long telomeres [mean telomere restriction fragment (TRF >30 kb, data not shown). Silver grain densities on terminal regions of chromosomes of CEM1301 after 24 h of culture with ^{3}H-360A were significantly greater than that calculated for the total metaphase area (*t*-test: $P < 0.0001$) (data not shown). Moreover, silver grain densities on terminal regions were also significantly higher than on the interstitial regions (Figure 4A and C). In contrast, the degraded sample of ^{3}H-360A did not exhibit such preferential localization in CEM1301 (Supplementary Figure 1B), as previously observed in T98G. These results thus confirmed the preferential accumulation of ^{3}H-360A at the ends of chromosomes. Interestingly, autoradiographs of CEM1301 cells that have very long telomeres did not show greater silver grain density at the ends of chromosomes than observed for T98G that have short telomeres (Figure 3E). Hence, the frequency of binding of ^{3}H-360A to chromosome termini does not appear to depend on telomere length.

Preferential binding of ^{3}H-360A to terminal regions of chromosomes in normal lymphocytes

We then treated PHA-activated PBL from a healthy donor with ^{3}H-360A for 24 h to investigate the binding of the compound in normal cells. Silver grain density was found again significantly higher at the ends of chromosomes than on the total metaphase area (*t*-test: $P < 0.0001$) and than on the interstitial regions (Figure 4B and C, *t*-test: $P < 0.0001$), indicating the preferential binding of the compound to terminal region of chromosomes from normal as well as cancer cells.

Preferential binding of ^{3}H-360A to terminal regions of the largest chromosomes in cells lines and PBL

To maximize resolution, we focused on the largest chromosomes: chromosome 1 of T98G and CEM1301, which is easy to identify in these highly rearranged cell lines, and chromosomes 1, 2 and 3 from normal PBL. The results (Table 2) showed that the frequencies of grains were systematically higher on terminal than on interstitial regions of these chromosomes after various times of treatment in the different cell types. These data, therefore, confirm preferential binding of the radioactive compound to chromosome ends. We also frequently detected grains over the heterochromatic region of the proximal long arm of chromosome 1, a region rich

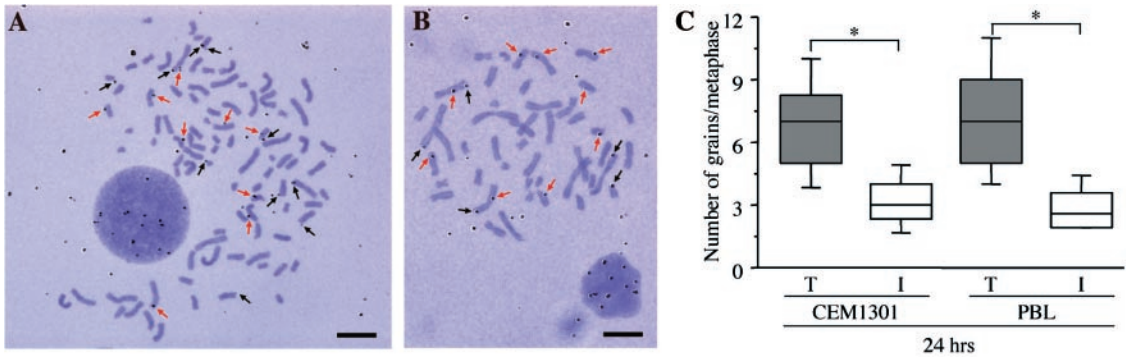

Figure 4. Autoradiographs of metaphase spreads from CEM1301 (**A**) and PBL (**B**) cultured with ^{3}H-360A. Cells were treated with ^{3}H-360A for 24 h. Black arrows indicate silver grains on the terminal regions and red arrows indicate grains on the interstitial regions. (**C**) Densities of silver grains on the terminal (*T*) and interstitial (*I*) regions of chromosomes on autoradiographs. Silver grains were counted in 50 metaphases/group. *I* values were normalized to areas of terminal regions by dividing the total numbers of grains in interstitial regions in each metaphase by the mean ratio of interstitial to terminal areas estimated with Metamorph software (CEM1301: 3.03 ± 0.44, $n = 12$; PBL: 3.64 ± 0.87, $n = 20$). Boxes include 50% of the values centered on the median (the horizontal line through the box). The vertical lines begin at the 10th percentile and end at the 90th percentile. *T* values are significantly greater than *I* values: *, *t*-test: $P < 0.0001$. Bars = 10 μm.

Table 2. Comparison between frequencies of silver grains on the terminal (FT) and interstitial (FI) regions of chromosomes 1, 2 and 3 in metaphase spreads of T98G cells, CEM1301 cells, and normal PBL treated with ^{3}H-360A

Cell	Time (h)	Chromosomes	Mean ratio of interstitial/terminal areas ± SD	Number of metaphases examined	Frequency of grains on terminal regions (FT)	Frequency of grains on interstitial regions (FI)	FT/FI
CEM1301	24	1	3.37 ± 0.65	50	0.120	0.056	2.14
T98G	24	1	4.10 ± 0.33	38	0.132	0.037	3.57
	48	1	4.10 ± 0.33	42	0.155	0.070	2.21
	72	1	4.10 ± 0.33	50	0.215	0.076	2.83
PBL1	24	1	5.98 ± 1.64	76	0.236	0.089	2.65
	24	2	5.21 ± 1.63	76	0.196	0.096	2.04
	24	3	4.26 ± 1.16	76	0.196	0.098	2.00
PBL2	72	1	5.11 ± 0.86	50	0.280	0.102	2.75
	72	2	4.43 ± 0.83	50	0.160	0.120	1.33
	72	3	3.35 ± 0.70	50	0.110	0.090	1.22

PBL were collected from two different donors (PBL1 and PBL2). Frequencies are given for 1 chromosome/metaphase. FI was calculated by dividing the frequency of silver grains on interstitial sequences by the mean ratio of interstitial areas versus terminal areas. Interstitial and terminal areas of chromosomes were estimated using Metamorph software (CEM1301: $n = 37$, T98G: $n = 35$, PBL: $n = 50$ for each donor).

Table 3. Higher frequencies of silver grains/10^6 bases on shorter than longer chromosomes, consistent with preferential binding of the G-quadruplex ligand to telomeres

Chromosomes	Chromosome length (bases × 10^6) (33)	Grains/10^6 bases
1	279	27.6
2	251	27.7
3	221	27.8
19 and 20	72 and 66	33.8
21, 22 and Y	45, 48 and 51	35.9

The silver grains on terminal and interstitial regions of chromosomes 1, 2 and 3 were separately numbered in 76 metaphases of normal PBL treated for 24 h with ^{3}H-360A. The frequencies of silver grains/10^6 bases were then deduced from the respective length of each chromosome. The same method was applied to the shorter chromosomes, except that chromosomes that were not easily distinguishable from each other by the technique used were analyzed together in two separate groups (chromosomes 19 and 20) and (chromosomes 21, 22 and Y).

in satellite DNAs, and over the long arm of chromosome 2, which contains interstitial telomeric sequences (data not shown).

Distribution of the grains in function of chromosome length consistent with a preferential binding to telomeres

We then investigated the hypothesis of a preferential binding of the compound to chromosome ends by another approach. We determined the frequency of silver grains per 10^6 bases found on some chromosomes (regardless of their location on those chromosomes) in metaphase spreads of normal PBL. Theoretically, if ^{3}H-360A binds preferentially to telomeres, the number of grains/10^6 bases should be greater for smaller chromosomes than for larger ones. On the contrary, if the compound does not preferentially bind to telomeres this frequency may either increase along with chromosome length (for instance if the compound has numerous binding sites elsewhere in the genome) or may vary independently of chromosome length (for instance if the number of binding sites depends on chromosomes or if these binding sites are localized specifically in terminal regions—but not in telomeres—of some particular chromosomes). We found that silver grain frequency (Table 3) was higher for the shortest chromosomes (19, 20, 21, 22 and Y) than for the longest chromosomes (1, 2 and 3). Therefore, this result confirms the preferential binding of the compound to terminal versus interstitial chromosome regions and suggests the existence of similar numbers of binding sites at all terminal regions of chromosomes. These data are thus in accordance with the hypothesis of a preferential binding of the compound to telomeres.

DISCUSSION

Here, we have shown that ^{3}H-360A accumulated in nuclei of cultured cells and was preferentially bound to terminal regions of chromosomes of human tumor and normal cells. Such predominant binding of this specific G-quadruplex ligand sustains the hypothesis for the *in vivo* formation of G-quadruplexes at telomeres of human cells.

In vitro selectivity of ^{3}H-360A for G-quadruplex structures

We checked selectivity for G-quadruplexes of ^{3}H-360A by competitive equilibrium dialysis and by hybridization experiments with human purified genomic DNA. The results obtained confirmed the potent selectivity of 360A toward G-quadruplex structures previously determined by equilibrium dialysis, FRET experiment or by TRAP-G4 assay (15). We found that the radioactive compound also interacted with the triplex samples in the competitive equilibrium dialysis assay. However, this was likely due to the disruption of triplexes by the ligand binding the purine-rich strands in a G-quadruplex conformation as suggested by control experiments without the pyrimidine oligomer that is required for triplex formation in this assay. Such an allosteric conversion into a different structure in the presence of a DNA ligand has already been observed for B–Z DNA (25). It should be noted that a similar behavior has been found for a number of strong quadruplex ligands (L. Guittat, personal communication): as the GA and GT triplexes are relatively easy to unfold (26), conversion to a different structure is possible.

Binding to terminal versus interstitial regions of chromosome in living cells

By comparing the densities of silver grains in autoradiographies of metaphase spreads, we found that ^{3}H-360A preferentially bound to terminal regions of chromosomes of two tumor cell lines (T98G and CEM1301) and also of normal PBL. The specificity of this binding was confirmed: (i) by the lack of such preferential localization of degraded compounds lacking affinity for G-quadruplex structures and (ii) by focusing on the localization of ^{3}H-360A on the largest chromosomes. Finally, the comparison of silver grain frequencies per chromosome sustained the hypothesis of a preferential localization of the compounds at terminal regions of all chromosomes. Our results do not rule out the possibility of specific binding sites located in interstitial sequences, such as in promoters of some specific genes (18). However, they indicate that a significant fraction of the binding sites of the compound is located at the terminal regions of chromosomes.

Binding sites of ^{3}H-360A at chromosomes ends

We showed by the comparison of CEM1301 and T98G that the binding of the compound to the terminal regions of chromosomes was not a simple function of telomere length as defined by mean TRF length determination. This is in agreement with *in vitro* data showing first that competition with a double-stranded telomeric oligonucleotide does not affect the ^{3}H-360A binding to genomic DNA and, second, that 360A very weakly binds to double-stranded telomeric repeats as compared with quadruplexes in a competitive dialysis experiment with a different set of sequences (data not shown).

Although the formation of G-quadruplex could occur all along the double-stranded telomeric DNA in particular circumstances (27,28), it is thought more likely to occur at the telomeric overhang because it does not necessitate the separation of the two strands of DNA, which could be unfavorable under physiological conditions (29). Such a preference for the telomeric G-overhang has been already reported for telomestatin, another G-quadruplex ligand (30–32). Our data showing that binding of ^{3}H-360A to terminal regions of chromosomes is independent of the double-stranded telomere length fit well with the hypothesis of a predominant binding to telomeric overhangs. Consistent with this hypothesis, *in vitro* hybridization and competition experiments on purified genomic DNA indicated that ^{3}H-360A has a preference for G-quadruplex structures formed by the telomeric overhang. However, we also showed in this assay that the ligand could bind to other sequences than the telomeric overhang. Such sites along telomeres and also G-rich subtelomeric sequences could thus contribute at least in part for the predominant localization of the compound at terminal regions of chromosomes found by autoradiography. They could possibly result from processes that require strands separation, such as DNA replication, that could allow the binding of the compound to G-quadruplex-forming elements on the single stranded DNA.

Binding of the G-quadruplex ligands to chromosome ends and cellular effects

We have shown elsewhere that the induction of apoptosis in immortalized cell lines by G-quadruplex ligands from our pyridine derivative series is related to multiple cell cycle alterations, including checkpoint activation, increase in metaphase duration and cytokenesis defects (15). All these effects are correlated with an induction of telomeric instability as shown by telomere-end fusion and anaphase bridge formation (15), indicating that these compounds act at telomeres. The data in the present study support the notion that the telomeric instability induced by G-quadruplexes interacting pyridine derivatives in immortalized cell lines is a direct consequence of the binding of the compounds to chromosome ends.

In conclusion, our results provide new evidences that a specific G-quadruplex ligand interacts with the terminal regions of chromosomes in human living cells. They support the hypothesis that G-quadruplex ligands induce and/or stabilize G-quadruplex structures at telomeres of human cells, at least in part at telomere overhang. We also found that this could occur in normal cells and immortalized cell lines. Interestingly, the non-radioactive form of our compound, 360A, has limited effects on proliferation of normal cells (C. Granotier *et al*., manuscript in preparation) as previously reported for telomestatin (12). 360A only slows the growth of normal PBL—without induction of apoptosis—and at higher concentrations than that required to induce apoptosis in tumor cell lines. We thus hypothesize that the binding of the compound to terminal region of chromosomes triggers different intracellular pathways between normal and tumor cells. All together, our results reinforce the hypothesis that G-quadruplexes may be formed at the ends of human chromosomes.

SUPPLEMENTARY MATERIAL

Supplementary Material is available at NAR Online.

ACKNOWLEDGEMENTS

The authors would like to thank T. Hercend (Sanofi-Aventis), D. Grierson (Institut Curie), L. Guittat (Muséum National d'Histoire Naturelle, Paris) and P. Fouchet (CEA) for scientific advices and O. Etienne (CEA) for technical assistance. This work was founded by SANOFI-AVENTIS and by an Action Concertée Incitative 'Médicament et Cibles thérapeutiques' from the Ministère de la Recherche et de la Technologie to J.-L.M., P.M., J.-F.R. and F.D.B., and by the ARC (##3365) to J.-L.M. and ARC (#3364) to J.-F.R. Funding to pay the Open Access publication charges for this article was provided by CEA/DSV/DRR/LRP.

Conflict of interest statement. None declared.

REFERENCES

1. Chan,S.W. and Blackburn,E.H. (2002) New ways not to make ends meet: telomerase, DNA damage proteins and heterochromatin. *Oncogene*, **21**, 553–563.
2. Shay,J.W. and Bacchetti,S. (1997) A survey of telomerase activity in human cancer. *Eur. J. Cancer*, **33**, 787–791.
3. Neidle,S. and Parkinson,G. (2002) Telomere maintenance as a target for anticancer drug discovery. *Nature Rev. Drug Discov*., **1**, 383–393.
4. Mergny,J.L., Riou,J.F., Mailliet,P., Teulade-Fichou,M.P. and Gilson,E. (2002) Natural and pharmacological regulation of telomerase. *Nucleic Acids Res*., **30**, 839–865.
5. Guittat,L., Alberti,P., Gomez,D., De Cian,A., Pennarun,G., Lemarteleur,T., Belmokhtar,C., Paterski,R., Morjani,H., Trentesaux,C.

et al. (2004) Targeting human telomerase for cancer therapeutics. *Cytotechnology*, **45**, 75–90.
6. Wang,Y. and Patel,D.J. (1993) Solution structure of the human telomeric repeat d[AG3(T2AG3)3] G-tetraplex. *Structure*, **1**, 263–282.
7. Parkinson,G.N., Lee,M.P. and Neidle,S. (2002) Crystal structure of parallel quadruplexes from human telomeric DNA. *Nature*, **417**, 876–880.
8. Neidle,S. and Parkinson,G.N. (2003) The structure of telomeric DNA. *Curr. Opin. Struct. Biol*., **13**, 275–283.
9. Gowan,S.M., Harrison,J.R., Patterson,L., Valenti,M., Read,M.A., Neidle,S. and Kelland,L.R. (2002) A G-quadruplex-interactive potent small-molecule inhibitor of telomerase exhibiting *in vitro* and *in vivo* antitumor activity. *Mol. Pharmacol*., **61**, 1154–1162.
10. Riou,J.F., Guittat,L., Mailliet,P., Laoui,A., Renou,E., Petitgenet,O., Megnin-Chanet,F., Hélène,C. and Mergny,J.L. (2002) Cell senescence and telomere shortening induced by a new series of specific G-quadruplex DNA ligands. *Proc. Natl Acad. Sci. USA*, **99**, 2672–2677.
11. Shammas,M.A., Shmookler Reis,R.J., Akiyama,M., Koley,H., Chauhan,D., Hideshima,T., Goyal,R.K., Hurley,L.H., Anderson,K.C. and Munshi,N.C. (2003) Telomerase inhibition and cell growth arrest by G-quadruplex interactive agent in multiple myeloma. *Mol. Cancer Ther*., **2**, 825–833.
12. Tauchi,T., Shin-ya,K., Sashida,G., Sumi,M., Nakajima,A., Shimamoto,T., Ohyashiki,J.H. and Ohyashiki,K. (2003) Activity of a novel G-quadruplex-interactive telomerase inhibitor, telomestatin (SOT-095), against human leukemia cells: involvement of ATM-dependent DNA damage response pathways. *Oncogene*, **22**, 5338–5347.
13. Incles,C.M., Schultes,C.M., Kempski,H., Koehler,H., Kelland,L.R. and Neidle,S. (2004) A G-quadruplex telomere targeting agent produces p16-associated senescence and chromosomal fusions in human prostate cancer cells. *Mol. Cancer Ther*., **3**, 1201–1206.
14. Burger,A.M., Dai,F., Schultes,C.M., Reszka,A.P., Moore,M.J., Double,J.A. and Neidle,S. (2005) The G-quadruplex-interactive molecule BRACO-19 inhibits tumor growth, consistent with telomere targeting and interference with telomerase function. *Cancer Res*., **65**, 1489–1496.
15. Pennarun,G., Granotier,C., Gauthier,L., Gomez,D., Hoffschir,F., Mandine,E., Riou,J., Mergny,J.L., Mailliet,P. and Boussin,F.D. (2005) Apoptosis related to telomere instability and cell cycle alterations in human glioma cells treated by new highly selective G-quadruplex ligands. *Oncogene*, **24**, 2917–2928.
16. Schaffitzel,C., Berger,I., Postberg,J., Hanes,J., Lipps,H.J. and Pluckthun,A. (2001) *In vitro* generated antibodies specific for telomeric guanine-quadruplex DNA react with *Stylonychia lemnae* macronuclei. *Proc. Natl Acad. Sci. USA*, **98**, 8572–8577.
17. Duquette,M.L., Handa,P., Vincent,J.A., Taylor,A.F. and Maizels,N. (2004) Intracellular transcription of G-rich DNAs induces formation of G-loops, novel structures containing G4 DNA. *Genes Dev*., **18**, 1618–1629.
18. Siddiqui-Jain,A., Grand,C.L., Bearss,D.J. and Hurley,L.H. (2002) Direct evidence for a G-quadruplex in a promoter region and its targeting with a small molecule to repress c-MYC transcription. *Proc. Natl Acad. Sci. USA*, **99**, 11593–11598.
19. Chang,C.C., Kuo,I.C., Ling,I.F., Chen,C.T., Chen,H.C., Lou,P.J., Lin,J.J. and Chang,T.C. (2004) Detection of quadruplex DNA structures in human telomeres by a fluorescent carbazole derivative. *Anal. Chem*., **76**, 4490–4494.
20. Lemarteleur,T., Gomez,D., Paterski,R., Mandine,E., Mailliet,P. and Riou,J.F. (2004) Stabilization of the c-myc gene promoter quadruplex by specific ligands' inhibitors of telomerase. *Biochem. Biophys. Res. Commun*., **323**, 802–808.
21. Rosu,F., De Pauw,E., Guittat,L., Alberti,P., Lacroix,L., Mailliet,P., Riou,J.F. and Mergny,J.L. (2003) Selective interaction of ethidium derivatives with quadruplexes: an equilibrium dialysis and electrospray ionization mass spectrometry analysis. *Biochemistry*, **42**, 10361–10371.
22. Dutrillaux,B. and Couturier,J. (1981) *La pratique de l'analyse chromosomique*. Masson, Paris.
23. Ren,J. and Chaires,J.B. (1999) Sequence and structural selectivity of nucleic acid binding ligands. *Biochemistry*, **38**, 16067–16075.
24. Guittat,L., Alberti,P., Rosu,F., Van Miert,S., Thetiot,E., Pieters,L., Gabelica,V., De Pauw,E., Ottaviani,A., Riou,J.F. *et al*. (2003) Interactions of cryptolepine and neocryptolepine with unusual DNA structures. *Biochimie*, **85**, 535–547.
25. Qu,X., Trent,J.O., Fokt,I., Priebe,W. and Chaires,J.B. (2000) Allosteric, chiral-selective drug binding to DNA. *Proc. Natl Acad. Sci. USA*, **97**, 12032–12037.
26. Mills,M., Arimondo,P.B., Lacroix,L., Garestier,T., Hélène,C., Klump,H. and Mergny,J.L. (1999) Energetics of strand-displacement reactions in triple helices: a spectroscopic study. *J. Mol. Biol*., **291**, 1035–1054.
27. Li,W., Miyoshi,D., Nakano,S. and Sugimoto,N. (2003) Structural competition involving G-quadruplex DNA and its complement. *Biochemistry*, **42**, 11736–11744.
28. Miyoshi,D., Matsumura,S., Nakano,S. and Sugimoto,N. (2004) Duplex dissociation of telomere DNAs induced by molecular crowding. *J. Am. Chem. Soc*., **126**, 165–169.
29. Phan,A.T. and Mergny,J.L. (2002) Human telomeric DNA: G-quadruplex, i-motif and Watson–Crick double helix. *Nucleic Acids Res*., **30**, 4618–4625.
30. Shin-ya,K., Wierzba,K., Matsuo,K., Ohtani,T., Yamada,Y., Furihata,K., Hayakawa,Y. and Seto,H. (2001) Telomestatin, a novel telomerase inhibitor from *Streptomyces anulatus*. *J. Am. Chem. Soc*., **123**, 1262–1263.
31. Kim,M.Y., Vankayalapati,H., Shin-ya,K., Wierzba,K. and Hurley,L.H. (2002) Telomestatin, a potent telomerase inhibitor that interacts quite specifically with the human telomeric intramolecular g-quadruplex. *J. Am. Chem. Soc*., **124**, 2098–2099.
32. Gomez,D., Paterski,R., Lemarteleur,T., Shin-ya,K., Mergny,J.L. and Riou,J.F. (2004) Interaction of telomestatin with the telomeric single-strand overhang. *J. Biol. Chem*., **279**, 41487–41494.
33. International Human Genome Sequencing Consortium. (2001) Initial sequencing and analysis of the human genome. *Nature*, **409**, 860–921.